Electron-nuclear double resonance of divalent holmium in calcium fluoride*

E. Secemski and W. Low
Microwave Division, The Racah Institute of Physics, The Hebrew University, Jerusalem, Israel
(Received 27 March 1973; revised manuscript received 9 November 1973)

The fluorine electron-nuclear-double-resonance (ENDOR) spectrum of Ho^{2+} in cubic sites in CaF_2 has been measured at 24 GHz. The analysis of the spectrum was complicated by the large magnitude of the hyperfine interaction. This caused the effective spin projection in the field direction, $\langle S_z \rangle$, to differ appreciably from $\pm 1/2$. The value of this reduced spin $\langle S_z \rangle$ was calculated from the eigenfunctions for each hyperfine state, obtained by diagonalization of the Hamiltonian. By using $\langle S_z \rangle$, it became possible to predict the ENDOR spectrum for all eight hyperfine levels, and also to specify uniquely to which m state each ENDOR transition belonged. This allowed absolute determination of sign and magnitude of the superhyperfine interaction constants for the first to the fourth nearest-neighbor F^- ions. For the first shell, $T_s = +3.54$ MHz, $T_p = -15.84$ MHz. Anomalies of the order of 1 MHz in the ENDOR frequencies were successfully accounted for by a superhyperfine pseudonuclear Zeeman effect. These results are discussed in relation to results on other rare-earth ions, and with respect to mechanisms for the superhyperfine interaction.

I. INTRODUCTION

Substitution of a trivalent rare-earth ion for the divalent calcium in CaF_2 usually involves some form of local-charge compensation, with a resultant loss of cubic symmetry. In some cases, however, it is possible to reduce the trivalent impurity ion to the divalent state, either electrolytically,[1] chemically,[2] or by x or γ radiation,[3] and so to restore the cubic symmetry of the site. This makes the spectrum and its interpretation much simpler. Such is the situation with holmium, which always enters CaF_2 as Ho^{3+} when grown by the Stockbarger method. On irradiation of the crystals, or on baking them in calcium vapor or treating them electrolytically, Ho^{2+} ions are formed by the capture of electrons by the Ho^{3+} ions, and the colorless crystal changes to blue. The symmetry of the Ho^{2+} is cubic, and the site is comparatively stable at room temperature.

The free Ho^{2+} ion has an electronic ground state $^4I_{15/2}$ $(4f^{11})$, and in the presence of a cubic field such as is found in CaF_2 the 16-fold degeneracy is split into two doublets, Γ_6 and Γ_7, and three Γ_8 quartets. It has been shown[4] that the ground state can be a Γ_6 or Γ_7 state, and in the case of CaF_2 the g factor proves that the ground state is the Γ_6 doublet. The nature of such a state is that it does not mix with any other Γ_7 or Γ_8 levels of different excited states, and hence can be regarded in the absence of a magnetic field as an isolated doublet. The g factor of such an isolated Γ_6 doublet in small magnetic field is negative, and should have the value -6.0. In the presence of a larger magnetic field, close-lying Γ_8 states mix in (in our case, only one of the Γ_8 levels being close enough for this) and the g factor could be expected to show some small deviation from -6.0.

The electron-paramagnetic-resonance (EPR) spectrum of cubic Ho^{2+} in CaF_2 has been independently investigated by Lewis and Sabisky[5] and by Hayes, Jones, and Twidell.[6] The spectrum appears at 4 °K and is isotropic, consisting of eight intense hyperfine lines, arising from the purely electronic $\Delta M = 0$ transitions, and a weaker seven-line structure arising from "forbidden" $\Delta M = \pm 1$ transitions. The spectrum can be fitted to a spin Hamiltonian of the form

$$\mathcal{H} = g\mu_B \vec{H} \cdot \vec{S} + A\vec{I} \cdot \vec{S} - g_N' \mu_N \vec{H} \cdot \vec{I}, \quad (1)$$

with $S = \frac{1}{2}$ and $I = \frac{7}{2}$. (Natural holmium contains only one isotope, Ho^{165}, which has $\frac{7}{2}$ nuclear spin.) For such an isolated Kramers doublet in a cubic field, g and A are scalars. g_N' is a pseudonuclear g factor introduced by Lewis and Sabisky to account for inconsistency in the fit of both the allowed and the forbidden transitions into the above spin Hamiltonian. The pseudonuclear g factor arises from the mixing of the ground Γ_6 doublet with the fairly-close-lying quartet Γ_8 state because of the unusually large hyperfine interaction. The best experimental fit was obtained by assigning the following values to the spin Hamiltonian parameters:

$$g = -5.912 \pm 0.003,$$

$$A = -(1307 \pm 3) \times 10^{-4}\ \text{cm}^{-1} = -3.921\ \text{GHz},$$

$$g_N' = +48.$$

Because of the extremely large magnitude of the hyperfine splitting, the full eight-line allowed spectrum is only observed if the exciting quantum is greater than about 18 GHz, and consequently the investigation to be reported here was made at K band, 24 GHz. At 9 GHz, two strong resonance lines are observed, only one of which is from an "allowed" transition.

Since the Ho^{2+} is surrounded by an octet of fluorine ions, it would be expected that there would be a superhyperfine interaction with these ligand ions. Any structure arising from this interaction was not apparent on the EPR spectrum, but the fact that the linewidths could not be reduced below about 10 G even at 1.6 °K suggested that inhomogeneous broadening was present.

This paper reports an ENDOR investigation on the complete allowed spectrum of the $CaF_2:Ho^{2+}$ cubic system. This is of particular interest because the very large hyperfine structure somewhat complicates the analysis of the ENDOR spectrum, but on the other hand permits unambiguous evaluation of the signs of the interaction constants. The constants so deduced are discussed in relation to the interaction mechanism, by comparison with results of other rare-earth ions.

II. THEORY–ENDOR SPECTRA

The main formulas used to interpret the ENDOR spectra have been vigorously derived for the general case by Zevin,[7] and for our specific case of a site of cubic symmetry by Ranon and Hyde.[8] The method of derivation will thus be only briefly indicated here.

Since the electronic Zeeman interaction is the largest term in the spin Hamiltonian, it is most convenient to work in a representation for which this term is diagonal. Thus, choosing the external field $\vec{H}$ to be along the [100] direction (the z axis), the spin Hamiltonian of the system, including the superhyperfine interaction with the nearest-neighbor fluorines, is

$$\begin{aligned}\mathcal{H} &= g\mu_B H S_z + A\vec{I}\cdot\vec{S} - g_N'\mu_N\vec{H}\cdot\vec{I} \\ &\quad + \sum_{i=1}^{8} (\vec{S}\cdot\overleftrightarrow{T}_i\cdot\vec{I}_i^F - g_N^F\mu_N\vec{H}\cdot\vec{I}_i^F) \\ &= \mathcal{H}_0 + \mathcal{H}_{\text{shf}} \ . \end{aligned} \tag{2}$$

The superhyperfine tensor T_i must be expressed in explicit form before the Hamiltonian can be diagonalized. It is most convenient for the interpretation of the ENDOR spectra to work with the axis of quantization of the superhyperfine Hamiltonian along the direction joining the fluorine ion with the Ho^{2+} ion, i.e., the body diagonal, z'. T_i will then be diagonal in this coordinate system and will have axial symmetry with components $T_\parallel$ along z' and $T_\perp$ in a plane perpendicular to z'. The superhyperfine part of $\mathcal{H}_{\text{shf}}$ then becomes

$$T_\parallel S_{z'} + T_\perp (S_{x'}I_{x'} + S_{y'}I_{y'}) \ .$$

$\mathcal{H}_{\text{shf}}$ can then be transformed to the unprimed coordinate system x, y, z in which $\mathcal{H}_0$ is expressed by means of a simple rotation. Since $\mathcal{H}_{\text{shf}}$ is so much smaller than $\mathcal{H}_0$, it can be regarded as a small perturbation of the hyperfine levels, and can be diagonalized separately.

However, because the magnitude of the hyperfine interaction $A\vec{I}\cdot\vec{S}$ is, in our case, large compared to the electronic Zeeman term $g\mu_B HS_z$, $\vec{S}$ will not be along $\vec{H}$, but will be along the resultant of $\vec{H}$ and the internal hyperfine field. Therefore, a reduced value $\langle S_z\rangle$ is introduced, which is the projection of $\vec{S}$ onto the $\vec{H}$ direction. The method of calculating $\langle S_z\rangle$ from $\mathcal{H}_0$ is given in Sec. III.

We thus have to diagonalize the nuclear spin Hamiltonian

$$\mathcal{H}_{\text{shf}} = \langle S_z\rangle \vec{T}\cdot\vec{I}^F - g_N^F\mu_N H I_z^F \ , \tag{3}$$

whence we obtain the eigenvalues for $I_Z = \pm\frac{1}{2}$:

$$\begin{aligned} E_F = \pm\tfrac{1}{2}[&(\langle S_z\rangle T_\parallel - g_N^F\mu_N H)^2\cos^2\theta \\ &+ (\langle S_z\rangle T_\perp - g_N^F\mu_N H)^2\sin^2\theta]^{1/2} \ . \end{aligned} \tag{4}$$

θ is here the angle subtended at the Ho^{2+} ion between $\vec{H}$ and the body diagonal.

The ENDOR transitions observed are between adjacent superhyperfine levels in the same $\langle S_z\rangle$ state. Thus, for a particular fluorine nucleus, we can write

$$\begin{aligned}(h\nu_N)^2 = &(\langle S_z\rangle T_\parallel - g_N^F\mu_N H)^2\cos^2\theta \\ &+ (\langle S_z\rangle T_\perp - g_N^F\mu_N H)^2\sin^2\theta \ , \end{aligned}$$

where ν_N is the ENDOR frequency. Using the notation of Ranon and Hyde,[8] and expressing all shf constants in MHz, this can be written as

$$\nu_N^2 = P^2\cos^2\theta + Q^2\sin^2\theta,$$

where

$$P = \langle S_z\rangle T_\parallel - \nu_0, \quad Q = \langle S_z\rangle T_\perp - \nu_0 \tag{5}$$

and ν_0 is the free F^- NMR frequency in field H.

Rearranging the expression, we have

$$\nu_N^2 = P^2 + (Q^2 - P^2)\sin^2\theta \ . \tag{6}$$

Thus a plot of ν_N^2 against $\sin^2\theta$ for any particular F^- ion should yield a pair of straight lines, one for $S_z = +\frac{1}{2}$ and one for $S_z = -\frac{1}{2}$ (high-field notation). From these lines, values of $|P|$ and $|Q|$ can be determined, but it is not possible to separate $\langle S_z\rangle T_\parallel$ and $\langle S_z\rangle T_\perp$ from ν_0 by means of an ENDOR measurement at a single setting of the external field. Furthermore, for an $S = \frac{1}{2}$ doublet, it is generally impossible to determine whether the positive or negative m state is being observed, so that extraction of absolute values of $T_\parallel$ and $T_\perp$ is impossible. In this experiment, however, ENDOR frequencies are measured for all eight hyperfine lines of the allowed EPR spectrum. This enables us to define uniquely whether the positive or negative m state is being observed, since a consistent fit of all eight lines is only possible in one of these two states. This technique also allows an absolute

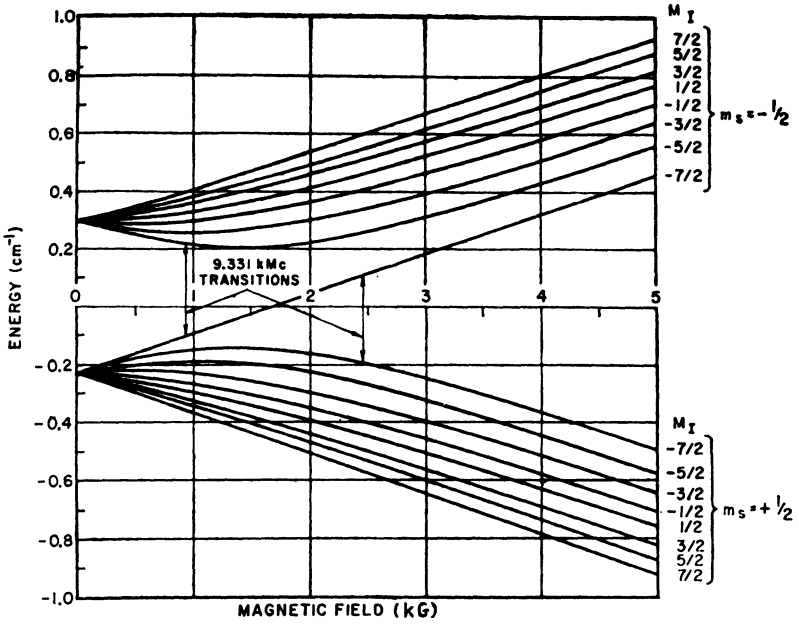

FIG. 1. Ground-state energy levels of divalent holmium in CaF_2 (taken from Ref. 5).

value of $\langle S_z\rangle T_\parallel$ to be determined from the two possibilities for $|P|$, and similarly for $\langle S_z\rangle T_\perp$ from $|Q|$. Consequently, an absolute determination of $T_\parallel$ and $T_\perp$ is possible.

III. HYPERFINE CALCULATION

In order to calculate the effective spin $\langle S_z\rangle$ for each hyperfine level, it is necessary to perform a full diagonalization of the spin Hamiltonian $\mathcal{H}_0$ [Eq. (1)].

Because of the off-diagonal elements in A, all but two (the $|\frac{1}{2},\frac{7}{2}\rangle$ and $|-\frac{1}{2},-\frac{7}{2}\rangle$ states) of the 16 hyperfine states are mixed spin states. The general form of the eigenfunction is

$$\Psi_{mM} = a\,|m, M\rangle + b\,|-m, M+2m\rangle\,. \tag{7}$$

The secular determinant reduces to a series of 2×2 determinants for the mixed states, giving the energy levels directly from a series of quadratic equations, the general solution of which is

$$E = -\tfrac{1}{4}A - g'_N\mu_N H(m+M) + m[16A^2 + (g\mu_B + g'_N\mu_N)^2H^2 + 2(m+M)A(g\mu_B + g'_N\mu_N)H]^{1/2}\,. \tag{8}$$

The energy levels are shown in Fig. 1 (taken from Lewis and Sabisky[5]). Insertion of these values of E into the Schrödinger equation for the eigenstate Ψ_{mM} and use of the normalization condition enables us to extract explicit expressions for a and b:

$$a^2 = \frac{-(G+g) - A(M+m) + X^{1/2}}{2X^{1/2}}\,,$$

$$b^2 = \frac{(G+g) + A(M+m) + X^{1/2}}{2X^{1/2}}\,,$$

where we have abbreviated

$$g\mu_B H = g,\quad g'_N\mu_N H = G\,,$$

and $X = 16A^2 + 2(m+M)A(g+G) + (g+G)^2$.

The expectation value of $\langle S_z\rangle$ for the state Ψ_{mM} is given by

$$\langle S_z\rangle_{mM} = \Big\langle a|m,M\rangle + b\,|-m,M+2m\rangle\Big| \times S_z\Big|a\,|m,M\rangle + b\,|-m,M+2m\rangle\Big\rangle\,.$$

Expanding, and applying the orthogonality condition for the set of states, we obtain

$$\langle S_z\rangle_{mM} = m(a^2 - b^2)\,.$$

Substituting values of a and b we obtain

$$\langle S_z\rangle_{mM} = \frac{-m[(g+G) + A(M+m)]}{[16A^2 + 2(M+m)A(G+g) + (g+G)^2]^{1/2}}\,. \tag{9}$$

As is observed, $\langle S_z\rangle_{mM}$ is a function of both m and M, as well as H, and so is different for each of the 14 mixed hyperfine states.

In our calculation, admixtures with the Γ_8 state were neglected. In principle, they can be taken care of in a similar way by using the correct $\Gamma_6 + \Gamma_8$ admixture for the wave function Ψ_{mM} in calculating $\langle S_z\rangle_{mM}$. In our case, this turns out to be negligibly small.

IV. EXPERIMENTAL METHOD

The experiments were performed on crystals containing nominally 0.05 mole% of Ho. These

TABLE I. Allowed EPR transitions at 23.70 GHz.

EPR transition $\|m, M\rangle \rightarrow \|-m, M\rangle$	Observed field (G)	Free fluorine NMR frequency ν_0 (MHz)	⟨100⟩ ENDOR line (MHz)
$\|\frac{1}{2}, -\frac{7}{2}\rangle \rightarrow \|-\frac{1}{2}, -\frac{7}{2}\rangle$	4390	17.60	22.00
$\|\frac{1}{2}, -\frac{5}{2}\rangle \rightarrow \|-\frac{1}{2}, -\frac{5}{2}\rangle$	3648	14.61	18.53
$\|\frac{1}{2}, -\frac{3}{2}\rangle \rightarrow \|-\frac{1}{2}, -\frac{3}{2}\rangle$	2972	11.91	15.56
$\|\frac{1}{2}, -\frac{1}{2}\rangle \rightarrow \|-\frac{1}{2}, -\frac{1}{2}\rangle$	2403	9.62	13.28
$\|\frac{1}{2}, \frac{1}{2}\rangle \rightarrow \|-\frac{1}{2}, \frac{1}{2}\rangle$	1933	7.75	11.50 (?)
$\|\frac{1}{2}, \frac{3}{2}\rangle \rightarrow \|-\frac{1}{2}, \frac{3}{2}\rangle$	1559	6.24	10.85
$\|\frac{1}{2}, \frac{5}{2}\rangle \rightarrow \|-\frac{1}{2}, \frac{5}{2}\rangle$	1277	5.11	10.69
$\|\frac{1}{2}, \frac{7}{2}\rangle \rightarrow \|-\frac{1}{2}, \frac{7}{2}\rangle$	1043	4.18	10.99

were mounted in a TE_{011} cylindrical cavity, in such a way as to permit rotation for alignment purposes during the experiment. The EPR system was a two-klystron superheterodyne system, operating at K band (24 GHz). A high degree of stability was achieved by electronically locking the signal-oscillator frequency to the cavity, and the local-oscillator frequency to the signal-oscillator frequency. The rf for the ENDOR was supplied by a Hewlett Packard HP8690 sweep oscillator, driving an Instruments for Industries wideband power amplifier delivering 10 W into 50 Ω. About $\frac{1}{2}$ G of rf field in the rotating frame was available at the crystal. The sensitivity of the whole spectrometer was such as to be able to display an ENDOR spectrum on the oscilloscope with a signal-to-noise ratio of the order of 10 in a sweep time of about 2 sec. This performance greatly facilitated alignment of the crystal.

No ENDOR spectra could be obtained at 4.2 °K, despite a strong EPR signal at this temperature, and it was necessary to work with pumped liquid helium. Even at this temperature, it was necessary to work with a high incident microwave power (of the order of 15 mW) to saturate the EPR lines and obtain good ENDOR spectra. This is in accordance with the spin-lattice relaxation-time measurements of Huang[9] who obtained a time as long as 1 msec only by going down to 2.8 °K. With the pumping system available, the temperature could be reduced to about 1.6 °K, and all spectra were plotted at this temperature.

A complete investigation of the ENDOR spectra with the external field along the three main crystal axes was performed on the highest-field hyperfine line. Additionally, one first-shell ENDOR

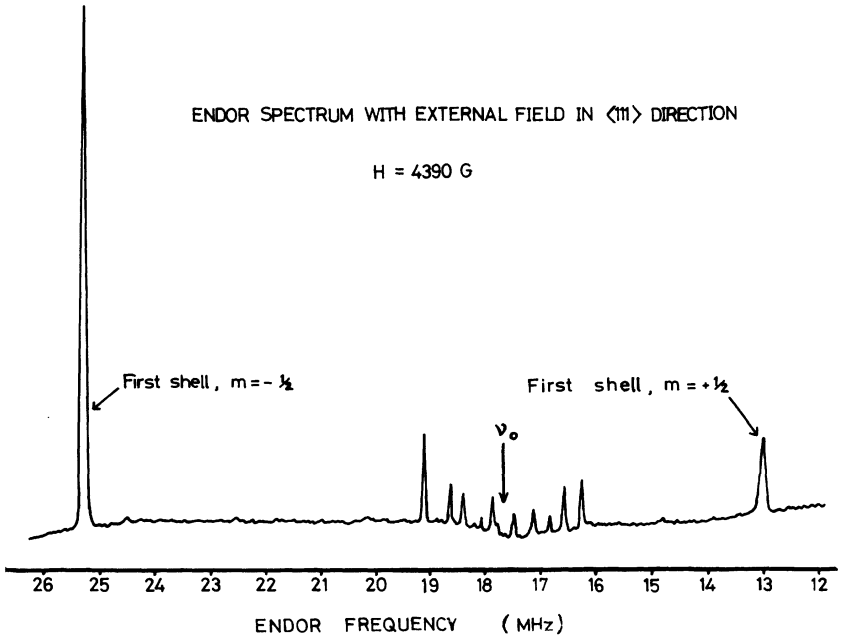

FIG. 2. ENDOR spectrum of highest hyperfine line with field in ⟨111⟩ direction.

TABLE II. First-shell ENDOR lines for main axis directions.

Mag. field orientation	$\sin^2\theta$	ν_n (MHz)
⟨100⟩	$\frac{2}{3}$	19.34, 22.00
⟨110⟩	1 or $\frac{1}{3}$	26.09, 26.76, 15.825
⟨111⟩	0 or $\frac{8}{9}$	13.00, 25.25

line of the ⟨100⟩ spectrum was measured for all eight hyperfine lines, in order to determine the absolute values of the superhyperfine components.

V. EXPERIMENTAL RESULTS

The EPR spectrum at 23.70 GHz is given in Table I, along with the infinite-field-notation labeling of each transition. The single ENDOR line plotted for all the hyperfine lines in also given. Because the EPR spectrum is isotropic, alignment of the crystal to one of the main axes required for each spectrum had to be performed by observing the ENDOR spectrum itself on the oscilloscope.

The spectra in the three main axis directions, ⟨100⟩, ⟨110⟩, and ⟨111⟩, were all typical of ENDOR spectra in CaF_2 systems, having a profusion of less intense lines grouped within about 2 MHz of the free fluorine NMR frequency in that particular field, and several intense individual lines farther away. The former are due to shf interactions with the second and farther shells of neighboring fluorine ions, while the latter are due to interaction with the first-shell (nearest-neighbor) fluorines. A recording of the spectra for the highest hyperfine line, with the field in the ⟨111⟩ direction, is shown in Fig. 2. The first-shell lines observed in the three principal axes, together with their angular origin, are given in Table II.

The 22.00-MHz line from the ⟨100⟩ spectrum was also measured for all eight hyperfine lines, and the results are shown in the last column of Table I.

VI. ANALYSIS OF RESULTS

It was not possible at the outset to determine which of the lines in Table II came from which of the two possible values of $\sin^2\theta$ (for ⟨110⟩ and ⟨111⟩), nor which of the lines were from the $m = +\frac{1}{2}$ and which from the $m = -\frac{1}{2}$ electronic state. However, on plotting ν_n^2 as a function of $\sin^2\theta$, as suggested by Eq. (6), it soon became apparent which of the ν_n's belonged to which straight line, and which value of $\sin^2\theta$ to assign to each. This is shown in Fig. 3. It also became evident from the graph that the two missing ⟨111⟩ ENDOR lines, and the one missing ⟨110⟩ line of Table II, fell outside the frequency range of our measurements. It was still not possible, however, to specify which m state to assign to each straight line.

From the graphs, the following mean values of $|P|$ and $|Q|$ were obtained:

$$|P|_+ = 4.41 \text{ MHz}, \quad |P|_- = 31.44 \text{ MHz};$$

$$|Q|_+ = 26.77 \text{ MHz}, \quad |Q|_- = 8.16 \text{ MHz};$$

where $|P|_+$, $|Q|_+$ are obtained from the straight line with positive slope, and $|P|_-$, $|Q|_-$ from that with negative slope.

From the sign ambiguity of $|P|_+$, there are two possible values of $T_\parallel$ for each m-state assignment, and similarly for $T_\perp$ from $|Q|_+$. Consequently, there are eight possible combinations of $T_\parallel$ and $T_\perp$, four from each m-state assignment. In order to determine which of these is the correct combination, we must use the ENDOR measurements made on all eight hyperfine EPR transitions.

First of all, the value of $\langle S_z \rangle$ is calculated for all of the 16 eigenstates, using Eq. (9). The values of A, g, and G are taken from Lewis and Sabisky.[5] The results are given in Table III.

Using Eqs. (5) and (6) and Table III, we now calculate the frequency of the ⟨100⟩ ENDOR line for the other hyperfine lines using each of the eight possibilities for $T_\parallel$ and $T_\perp$. We then compare these predicted frequencies with the observed frequencies of this line, as given in the last column

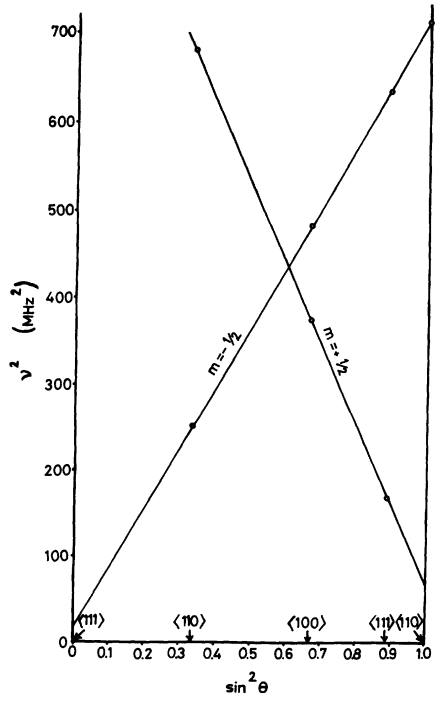

FIG. 3. First-shell ENDOR frequencies as a function of θ, the angle between the external field direction and the body diagonal.

TABLE III. Values of $\langle S_z \rangle$ for eigenstates at 23.70 GHz.

Eigenstate Ψ_{mM}	$\langle S_z \rangle_{mM}$	Eigenstate Ψ_{mM}	$\langle S_z \rangle_{mM}$
$\vert -\frac{1}{2}, -\frac{7}{2}\rangle$	−0.500	$\vert \frac{1}{2}, -\frac{7}{2}\rangle$	0.460
$\vert -\frac{1}{2}, -\frac{5}{2}\rangle$	−0.435	$\vert \frac{1}{2}, -\frac{5}{2}\rangle$	0.427
$\vert -\frac{1}{2}, -\frac{3}{2}\rangle$	−0.387	$\vert \frac{1}{2}, -\frac{3}{2}\rangle$	0.402
$\vert -\frac{1}{2}, -\frac{1}{2}\rangle$	−0.363	$\vert \frac{1}{2}, -\frac{1}{2}\rangle$	0.392
$\vert -\frac{1}{2}, \frac{1}{2}\rangle$	−0.356	$\vert \frac{1}{2}, \frac{1}{2}\rangle$	0.397
$\vert -\frac{1}{2}, \frac{3}{2}\rangle$	−0.371	$\vert \frac{1}{2}, \frac{3}{2}\rangle$	0.418
$\vert -\frac{1}{2}, \frac{5}{2}\rangle$	−0.402	$\vert \frac{1}{2}, \frac{5}{2}\rangle$	0.453
$\vert -\frac{1}{2}, \frac{7}{2}\rangle$	−0.445	$\vert \frac{1}{2}, \frac{7}{2}\rangle$	0.500

of Table I.

In Table IV this comparison procedure is shown in full for the second hyperfine line ($M = -\frac{5}{2}$) for all eight possibilities. It is apparent just from this line that option (h) is the correct combination, and that the positive sloped line in Fig. 3 is due to the negative m-state ENDOR transitions. In Table V, the frequencies of the negative m-state ⟨100⟩ ENDOR line for all eight hyperfine lines, calculated using option (h), are compared with the experimental values. The agreement, as observed, is excellent and within the experimental error attributed to each line. (The $M = \frac{1}{2}$ line seems to have been incorrectly measured.) None of the other possible combinations of $T_\parallel$ and $T_\perp$ showed any semblance of fit to all the measured hyperfine lines.

The superhyperfine coupling constants have thus been uniquely determined in this experiment, having apparent values $T_\parallel = -26.38$ MHz, $T_\perp = 18.30$ MHz.

VII. ENDOR TRANSITION INTENSITIES

A further check on the identification of the m state involved in each transition, and on the sign of $T_\parallel$ and $T_\perp$, is given by an inspection of the relative intensity of the ENDOR lines for positive and negative m-state transitions. It had already been noted that the ENDOR transitions on the positive-sloped line of Fig. 3 (negative m) were consistently more intense than the corresponding transitions on the negative-sloped line. Davies and Reddy[10] have deduced formulas for the relative intensities of the two m-state ENDOR transitions. For the ⟨111⟩ spectra, in which direction $\tilde{T}$ is diagonal, and for isotropic g, the intensity I_m is proportional to $(1 - mT_\perp/\nu_0)^2$. Substituting $T_\perp = 18.3$ MHz, $\nu_0 = 17.6$ MHz, and $m = +0.46$ or -0.50, we obtain $I_-/I_+ = 8.5$. Assuming that the rf field output is uniform over the frequency range used, a comparison of the intensities of the two ⟨111⟩ spectra first-shell lines in Fig. 2 showed that $I_{\nu=25.25}/I_{\nu=13.00} \approx 8.0$, thereby confirming that the 25.25-MHz line is from the negative m-state transition, and the 13.00-MHz line from the positive transition.

VIII. SUPERHYPERFINE PSEUDONUCLEAR ZEEMAN INTERACTION

The values of $T_\parallel$ and $T_\perp$ derived above, and all the subsequent fitting to the lower hyperfine lines, were obtained from P_+ and Q_+, i.e., from the negative m state, $\langle S_z \rangle = -0.5$. Upon attempting to fit the positive m-state ENDOR lines to the values of $T_\parallel$ and $T_\perp$ obtained, using $\langle S_z \rangle = +0.46$, it was found that the fit was far outside the probable experimental error, having apparent values $T_\parallel = -30.10$ MHz, $T_\perp = 20.50$ MHz. However, the fact that two good straight lines were obtained in Fig. 3 indicates that the origin of this deviation has the same symmetry as the superhyperfine interaction itself, and can thus be included as a simple correction to Eq. (5).

The deviation is best described experimentally by the mutual shift in ENDOR frequencies for the orientations $\sin^2\theta = 1$ and 0, since at these two alignments the magnetic field is perpendicular and parallel, respectively, to the ligand direction, and so the frequencies are defined in terms of $T_\perp$ and $T_\parallel$ alone, respectively. From Eq. (5) it is seen that at these two points the "center of gravity" of the two ENDOR frequencies from each m state should

TABLE IV. Comparison of predicted ENDOR line with measured line for second hyperfine line ($\vert \frac{1}{2}, -\frac{5}{2}\rangle$ to $\vert -\frac{1}{2}, -\frac{5}{2}\rangle$).

		$T_\parallel$ (MHz)	$T_\perp$ (MHz)	ν_N calculated (MHz)	ν_N measured
Positive	(a)	47.92	96.50	21.9	
m state	(b)	47.92	−19.92	19.15	
$\langle S_z \rangle = 0.427$	(c)	28.65	96.50	21.7	
	(d)	28.65	−19.92	18.9	
Negative	(e)	−44.02	−88.70	19.8	18.53 MHz ±20 kHz
m state	(f)	−44.02	18.30	18.62	
$\langle S_z \rangle = -0.435$	(g)	−26.38	−88.70	19.7	
	(h)	−26.38	18.30	18.52	

TABLE V. Comparison of measured negative m-state $\langle 100\rangle$ ENDOR frequency with calculated value for all eight hyperfine lines.

Hyperfine line (M value)	ν calculated (MHz)	ν measured (MHz)
$-\frac{7}{2}$	22.00	22.00
$-\frac{5}{2}$	18.52	18.53
$-\frac{3}{2}$	15.56	15.56
$-\frac{1}{2}$	13.29	13.28
$\frac{1}{2}$	11.75	11.50 (?)
$\frac{3}{2}$	10.88	10.85
$\frac{5}{2}$	10.67	10.69
$\frac{7}{2}$	10.98	10.99

fall at ν_0, the free fluorine NMR frequency in our field H. In fact, there is a shift in this center of gravity which is of opposite sign for the parallel and perpendicular orientations. In place of Eq. (5) we can write

$$(\nu_\perp)_\pm = |\langle S_z\rangle_\pm T_\perp - \nu_0 - \Delta\nu_\perp| \quad \text{for } \langle 110\rangle ,$$

$$(\nu_\parallel)_\pm = |\langle S_z\rangle_\pm T_\parallel - \nu_0 - \Delta\nu_\parallel| \quad \text{for } \langle 111\rangle ,$$

where $\nu_\pm$ are the two ENDOR frequencies at each alignment. Substituting values for ν and eliminating $T_\parallel$ and $T_\perp$, we obtain for the experimental shifts that $\Delta\nu_\perp = -520$ kHz and $\Delta\nu_\parallel = 875$ kHz.

The fact that the ratio $\Delta\nu_\perp : \Delta\nu_\parallel \approx -1:2$ suggests that the origin of the shift is magnetic dipolar in form. Also, the fact that the deviation could be fully described by shifts in the value of $\nu_0 = g_N^F \mu_N H$ pointed to an explanation based on some sort of pseudonuclear g factor.[11]

As mentioned above,[5,12] a pseudonuclear g factor is present for the holmium nucleus because cross terms between the Ho hyperfine interaction and the electron Zeeman interaction mix the excited Γ_8 state into the Γ_6 ground state. In an exactly analogous manner, the superhyperfine interaction can give rise to a pseudonuclear g factor for the fluorine ion. Since the superhyperfine interaction is so much smaller than the central-ion hyperfine interaction, the energy shift will be much smaller, and will generally only be detected on the ENDOR spectrum.

The perturbation to the Hamiltonian for the ground manifold of the free ion can be written as

$$\begin{aligned}\Delta\mathcal{H} &= -\sum_j \frac{\langle\Gamma_6|\vec{t}\cdot\vec{I}|\Gamma_{8j}\rangle\langle\Gamma_{8j}|\mu_B(\vec{L}+2\vec{S})\cdot\vec{H}|\Gamma_6\rangle + \text{c.c.}}{E(\Gamma_{8j}) - E(\Gamma_6)} \\ &= -\sum_{pq}\sum_j \frac{\langle\Gamma_6|t_p|\Gamma_{8j}\rangle\langle\Gamma_{8j}|\mu_B(L+2S)_q|\Gamma_6\rangle + \text{c.c.}}{E(\Gamma_{8j}) - E(\Gamma_6)} I_p H_q \\ &= -\sum_{pq} \Delta g_{pq}\,\mu_N I_p H_q \quad \text{by definition} . \end{aligned} \tag{10}$$

The superhyperfine pseudonuclear g factor is defined by $(g_N^F + \Delta g_{pq})$, where pq are components of the cubic x, y, z, coordinate system. The correction Δg_{pq} has the same symmetry as the superhyperfine interaction, and so is anisotropic (in contrast to the central-ion pseudonuclear effect for a cubic site). In Eq. (10) j labels the various Γ_8 excited states and $\vec{t}$ is the free-ion superhyperfine interaction constant.

The calculation consists of three stages. First, an operator equivalent of the superhyperfine interaction must be constructed in order to calculate the matrix elements $\langle\Gamma_6|\vec{t}_p|\Gamma_{8j}\rangle$. Then, the electronic Zeeman matrix elements $\langle\Gamma_{8j}|\mu_B(L+2S)_q|\Gamma_6\rangle$ are calculated using the eigenfunctions given by Lea, Leask, and Wolf.[4] Finally, a geometrical transformation is performed to convert the pq coordinates of Eq. (10) to the axial system in which $T_\parallel$ and $T_\perp$ are measured. Details of the calculation are given elsewhere by Zevin *et al.*[11] The result is obtained for cubic symmetry that

$$\begin{aligned} \Delta g_{zz} &= 0 , \\ \Delta g_{zx} &= \frac{2 g_N^F g_J^2 \mu_B^2}{R^3} \sum_j \frac{|\langle\Gamma_6|J_x|\Gamma_8\rangle|^2}{E(\Gamma_{8j}) - E(\Gamma_6)} , \end{aligned} \tag{11}$$

where

$$\begin{aligned} \Delta g_{zz} &= \tfrac{1}{3}(\Delta g_\parallel + 2\Delta g_\perp) , \\ \Delta g_{zx} &= \tfrac{1}{3}(\Delta g_\parallel - \Delta g_\perp) . \end{aligned} \tag{12}$$

g_J is here the Landé g factor for the holmium ion and R is the distance between the central-ion nucleus and the ligand nucleus.

The energy-level diagram for Ho^{2+} in CaF_2 has been obtained from optical measurements by Weakliem and Kiss.[13] Their results show that the lowest of the three Γ_8 quartets predicted by the cubic crystal field splitting lies only 33.8 cm^{-1} above the Γ_6 ground state. The other Γ_8 states are about an order of magnitude higher in energy, and so

their admixture may be neglected in the summation in Eqs. (11). From the tables of eigenfunctions given by Lea, Leask, and Wolf[4] for $J=\frac{15}{2}$ in cubic crystal field, one can obtain the value of the matrix element $\langle\Gamma_6|J_x|\Gamma_8^{(1)}\rangle=3.72$. Inserting this into Eqs. (11) and (12), and using the values $g_J=\frac{6}{5}$, $R=2.36$ Å, and $E(\Gamma_8^{(1)})-E(\Gamma_6)=33.8\ \mathrm{cm}^{-1}$, we obtain $\Delta\nu_\perp=-675$ kHz and $\Delta\nu_\parallel=1350$ kHz. These values thus agree fairly well with the experimentally determined frequency shifts. The major approximation made in the derivation is that the point-charge model of the crystal field holds and that the wave functions of Lea, Leask, and Wolf[4] are thus an adequate description. In fact, it is known that there is a considerable covalent contribution to the superhyperfine interaction—about 20% of the total, as shown below. However, the superhyperfine interaction itself involves only matrix elements within the Γ_6 ground state, while the superhyperfine pseudonuclear Zeeman interaction involves matrix elements between the Γ_6 and the excited Γ_8 state. Extrapolation of the effect of covalency to such a mixed-state situation is difficult to predict, and must await further calculations, but it seems not unreasonable to be able to account for most of our discrepancy in the shf pseudonuclear effect in this way. Further minor approximations made in the derivation of the shf pseudonuclear effect are discussed by Zevin *et al.*[11]

When the superhyperfine pseudonuclear connection is taken into account, the values of $T_\parallel$ and $T_\perp$ from both m states are calculated consistently as $T_\parallel=-28.13$ MHz and $T_\perp=19.38$ MHz.

IX. PHYSICAL INTERPRETATION OF $T_\parallel$ AND $T_\perp$

The representation of T_i in terms of $T_\parallel$ and $T_\perp$ is simply an outcome of the axial symmetry of the superhyperfine interaction along the bond axis, and in this respect no physical meaning has been attached to $T_\parallel$ and $T_\perp$. If we define two new shf coefficients

$$T_s=\tfrac{1}{3}(T_\parallel+2T_\perp),\quad T_p=\tfrac{1}{3}(T_\parallel-T_\perp),$$

and substitute into Eq. (2), the superhyperfine part of $\mathcal{H}_{\mathrm{shf}}$ can be written as

$$T_s\vec{\mathrm{S}}\cdot\vec{\mathrm{I}}^{\mathrm{F}}+T_p(3S_zI_z^{\mathrm{F}}-\vec{\mathrm{S}}\cdot\vec{\mathrm{I}}^{\mathrm{F}}).$$

This form has been obtained simply by defining new interaction constants, T_s and T_p, and as such is as generally applicable for all problems of axial symmetry as are $T_\parallel$ and $T_\perp$. It is noted, however, that the Hamiltonian is now expressed as the sum of two parts—an isotropic term involving T_s and an anisotropic term, with T_p traceless, having the same form as the classical dipole-dipole interaction between the Ho^{2+} electrons and the F^- ligand nucleus. Now, in an S-state ion, the diagonal tensor T_s arises only from unpairing of the $1s$ and $2s$ electrons on the ligand as a result of direct bonding and polarizing effects,[14] while T_p is the sum of the contributions of the dipole interaction and of the unpairing of the $2p\sigma$ and $2p\pi$ electrons on the ligand. For a non-S-state ion, however, the p electrons contribute to both T_s and T_p in a manner which depends in a complicated way on the covalency admixture parameters and the overlap integrals for the various orbitals involved.[15] It is instructive, and accepted practice, to continue to use T_s and T_p in their simpler roles, as a first-order approximation in the absence of a full molecular-orbital treatment of the covalency. This representation also enables us to subtract out the dipolar interaction, giving us the covalent contribution directly. Substituting, we obtain $T_s=3.54$ MHz and $T_p=-15.84$ MHz. The experimental uncertainty in T_s and T_p is ± 30 kHz.

The dipolar contribution is given by

$$T_{d\text{-}d}=g\mu_B g_N^{\mathrm{F}}\mu_N/R^3,$$

where R is the $Ho^{2+}-F^-$ internuclear distance. Assuming an undistorted lattice, the dipolar contribution to T_p comes out to be -16.80 MHz. Consequently, the covalent contributions to the shf interaction are $T_s=3.54$ MHz and $T_p=0.96$ MHz.

X. SECOND AND FURTHER FLUORINE SHELLS

By substituting T_s and T_p into Eqs. (5) and (6) and rearranging, the ENDOR frequencies can be written as

$$\nu_N^2=\{\nu_0-\langle S_z\rangle[T_s+T_p(3\cos^2\theta-1)]\}^2+9\langle S_z\rangle^2T_p^2\cos^2\theta\sin^2\theta\ . \tag{13}$$

For the second and more distant fluorine shells, ν_0 is expected to be the dominant term, and so expression (13) can be expanded binomially, giving

$$\nu=\nu_0-\langle S_z\rangle[T_s+T_p(3\cos^2\theta-1)]+\frac{\langle S_z\rangle^2}{2\nu_0}\times\{[T_s+T_p(3\cos^2\theta-1)]^2+9T_p^2\cos^2\theta\sin^2\theta\}. \tag{14}$$

It is observed that since $\langle S_z\rangle$ is different in magnitude for the positive and negative m-state transitions, the second and farther shell lines are not expected to fall symmetrically on either side of ν_0, even in the first-order approximation. This is the case if $S_z=\pm\frac{1}{2}$ exactly. This feature of the theory enables us to define which of the two ENDOR lines arising from each set of equivalent fluorines is associated with which m state. In this way, the absolute signs of the interaction constants are determined, instead of having to be assigned by comparison with the sign of the dipolar interaction, as is usually done.

TABLE VI. Superhyperfine interaction coefficients for first four shells (all components in MHz).

Shell	T_s (obs)	T_p (obs)	T_{d-d} (calc)
1	$+3.54 \pm 0.02$	-15.84 ± 0.02	-16.80
2	$+0.02 \pm 0.01$	-2.360 ± 0.01	-2.390
3	0.00 ± 0.01	-1.043 ± 0.01	-1.052
4	0.00 ± 0.01	-0.620 ± 0.01	-0.621

In order to determine rough initial values of T_s and T_p, the first-order approximation [Eq. (14)] is sufficient. The spacing between the two lines ν_+ and ν_- arising from each set of equivalent fluorines is thus given by

$$\nu_+ - \nu_- = [\langle S_z \rangle_+ - \langle S_z \rangle_-][T_s + T_p(3\cos^2\theta - 1)] . \quad (15)$$

For the highest-field hyperfine line (on which all the second- and farther-shell measurements were performed), we have

$$\langle S_z \rangle_+ = +0.46, \quad \langle S_z \rangle_- = -0.50 .$$

Substituting in (15), values for T_s and T_p were calculated for the second, third, and fourth shells from the relatively simple ⟨100⟩ spectrum. Using these values, all the lines of the ⟨100⟩ and ⟨111⟩ spectra could also be identified, and the final values of T_s and T_p for each shell were obtained by performing a least-squares fit of the calculated lines with those measured. These values, together with those for the first shell, are given in Table VI, where the dipolar contribution assuming an undistorted lattice is also given. As expected from the results of measurements on other rare-earth ions in cubic sites, the small difference between T_p and T_{d-d} for the third and fourth shells indicates that there is negligible bonding at this distance. Moreover, the assumed distance for calculation of T_{d-d} is shown to be good.

XI. DISCUSSION

In order to comment on the results obtained for the covalent contribution to the superhyperfine interaction for the first-shell fluorines, it is first necessary to consider some of the mechanisms proposed for the origin of this interaction.

The interaction itself arises from the excess spin density set up at the nucleus of the normally diamagnetic F^- ion, by polarization of the normally closed $1s$, $2s$, and $2p$ orbitals. As mentioned above, there are two opposing mechanisms operating to cause this polarization.

(i) Direct overlap of the f electrons onto the ligand orbitals, which would produce a parallel polarization, i.e., unpaired electron spin density at the F^- nucleus in the same direction as the net spin of the paramagnetic metal ion.

(ii) Several proposed mechanisms that would give an antiparallel polarization of the ligand electrons, i.e., a negative spin density. The simplest of these is the core-polarization mechanism of Watson and Freeman,[14] in which the nominally closed shells of the paramagnetic ion are exchange polarized by the unpaired f electrons to yield a net antiparallel spin density at the outer reaches of the ion. This then overlaps with the ligand orbitals, thus causing an antiparallel polarization in them. Another such mechanism has been proposed by Lewis *et al.*[16] involving transfer of an electron from the ligand into an unoccupied $6s$ shell of the metal ion—an extension of the configuration-interaction mechanism of Shulman and Jaccarino.[17]

The interpretation of the results depends on the correct assessment of these two opposing sources of the F^- orbitals' polarization. In the S-state ions of the rare-earth series, the calculations of Freeman and Watson suggested that the dominant mechanism is indeed the core-polarization effect, which is about ten times greater in magnitude than the direct contribution from the $4f$ electrons. Subsequent ENDOR measurements on Eu^{2+} [18] and Gd^{3+} [19] have confirmed these predictions both in sign and approximate magnitude. Extrapolation of these results to other rare-earth ions is rather difficult.

The problem has been discussed by Baker[15] in connection with the result on Tm^{2+} and Yb^{3+} ($4f^{13}$). For Tm^{2+}, which is more directly comparable, the results are[20]

$$T_s = +2.58 \text{ MHz}, \quad T_p = +2.47 \text{ MHz} ;$$

i.e., the signs and magnitudes are similar to those of Ho^{2+}. The important feature is that the sign of the interaction is positive, indicating a parallel polarization. Thus, the situation has changed in going from the $4f^7$ configuration to the $4f^{11}$ and $4f^{13}$ configurations. Since the effect of direct $4f$ polarization is not expected to alter much, the change must be sought in a drastic reduction of the core polarization at the ligand. Failing any exact calculations, this can only be surmised at by means of reasoned arguments. Calculations by Watson *et al.*[21] indicate that the s-electron core polarization at the nucleus of the rare earth decreases steadily through the group from Ce^{3+} to Yb^{3+}, reaching zero effectively at Yb^{3+}. However, this is the net effect at the nucleus of all of the s-shells, while the superhyperfine interaction depends primarily on the polarization of the $5p$ subshell. In the absence of any more definitive information, it may be reasonable to assume that the core polarization varies with the real spin of the ion (as for the $3d$ group). Thus, in going from $4f^7$ to $4f^{11}$ (and $4f^{13}$) not only is the net spin producing the polarization in the $5p$ shell smaller,

but the overlap itself between the $4f$ and the $5p$ is smaller, so that we would expect a greatly diminished core-polarization effect. This, combined with the approximate constancy of the $4f$ positive polarization at the ligand, may well explain the sign change in going from Gd^{3+} to Ho^{2+}. However, this would require the parallel $4f$ polarization to be significant in both cases, much larger than had been previously assumed. This explanation is therefore not entirely satisfactory. A full understanding of the magnitude of the superhyperfine interaction must await detailed covalency calculations.

ACKNOWLEDGMENTS

The authors gratefully acknowledge the hospitality of Professor B. Elschner of the II Physikalische Institut of the Technischen Hochschule, Darmstadt, where the experiments were performed, and thank W. Rhein and R. Valentin of the Institut for their assistance during the course of the experiment. The authors would also like to thank Dr. V. Zevin for many helpful discussions and in particular for suggesting this method for calculating $\langle S_z \rangle$. The crystal was generously supplied by E. S. Sabisky of R. C. A. Laboratories, Princeton.

---

*This research sponsored in part by the U. S. Department of Commerce, National Bureau of Standards, under Grant No. NBS (G) 118. In the last stage supported in part by the Stiftung Volkswagenwerk.

[1]H. Guggenheim and J. V. Kane, Appl. Phys. Lett. 4, 172 (1964); F. K. Fong, J. Chem. Phys. 41, 2291 (1964).

[2]Z. J. Kiss and P. N. Yokum, J. Chem. Phys. 41, 1507 (1964).

[3]Z. J. Kiss, Phys. Rev. 127, 718 (1962).

[4]K. R. Lea, M. J. M. Leask, and W. P. Wolf, J. Phys. Chem. Solids 23, 1381 (1962).

[5]H. R. Lewis and E. S. Sabisky, Phys. Rev. 130, 1370 (1963); E. S. Sabisky, Phys. Rev. 141, 352 (1966).

[6]W. Hayes, G. D. Jones, and J. W. Twidell, Proc. Phys. Soc. Lond. 81, 371 (1963).

[7]V. Zevin, Phys. Lett. 43A, 386 (1973).

[8]U. Ranon and J. S. Hyde, Phys. Rev. 141, 259 (1966).

[9]Chao-Yuan Huang, Phys. Rev. 139, A241 (1965).

[10]E. R. Davies and T. Rs. Reddy, Phys. Lett. 31A, 398 (1970).

[11]V. Zevin, E. Secemski, and W. Low (unpublished).

[12]J. M. Baker and B. Bleaney, Proc. R. Soc. A245, 156 (1958).

[13]H. A. Weakliem and Z. J. Kiss, Phys. Rev. 157, 277 (1967).

[14]R. E. Watson and A. J. Freeman, Phys. Rev. Lett. 6, 277 (1961).

[15]J. M. Baker, J. Phys. C 1, 1670 (1968).

[16]W. B. Lewis, J. A. Jackson, J. F. Lemons, and H. Taube, J. Chem. Phys. 36, 694 (1962).

[17]R. G. Shulman and V. Jaccarino, Phys. Rev. 108, 1219 (1957).

[18]K. Baberschke, Phys. Lett. 34A, 41 (1971).

[19]H. Bill, Phys. Lett. 29A, 593 (1969).

[20]R. G. Bessent and W. Hayes, Proc. R. Soc. A285, 430 (1965).

[21]R. E. Watson, P. Bagus, and A. J. Freeman, Bull. Am. Phys. Soc. 13, 484 (1968).